AD-A075 206 HARRY DIAMOND LABS ADELPHI MD F/G 13/7
A FLUIDIC APPROACH TO THE DESIGN OF A MUD PULSER FOR BORE-HOLE --ETC(U)
AUG 79 A B HOLMES, S E GEHAMAN
UNCLASSIFIED HDL-TM-79-21 NL

1 OF 2
ADA 075206

END
DATE FILMED
11-79
DDC

CONT

LEVEL II

HDL-TM-79-21
August 1979

A Fluidic Approach to the Design of a Mud Pulser for Bore-Hole Telemetry While Drilling

by Allen B. Holmes
Stacy E. Gehman

U.S. Army Electronics Research and Development Command
Harry Diamond Laboratories
Adelphi, MD 20783

This research is sponsored by the U.S. Geological Survey, Research and Development Program for OCS Oil and Gas Operations, under Technology Transfer Authorization.

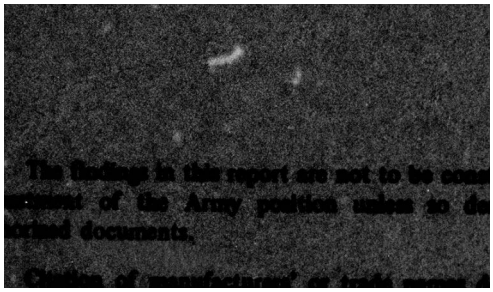

UNCLASSIFIED

SECURITY CLASSIFICATION OF THIS PAGE (When Data Entered)

REPORT DOCUMENTATION PAGE

READ INSTRUCTIONS BEFORE COMPLETING FORM

1. REPORT NUMBER: HDL-TM-79-21	2. GOVT ACCESSION NO.
3. RECIPIENT'S CATALOG NUMBER	
4. TITLE (and Subtitle): A Fluidic Approach to the Design of a Mud Pulser for Bore-Hole Telemetry While Drilling.	5. TYPE OF REPORT & PERIOD COVERED: Technical Memorandum
6. PERFORMING ORG. REPORT NUMBER	
7. AUTHOR(s): Allen B. Holmes; Stacy E. Gehman	8. CONTRACT OR GRANT NUMBER(s): 40
9. PERFORMING ORGANIZATION NAME AND ADDRESS: Harry Diamond Laboratories, 2800 Powder Mill Road, Adelphi, MD 20783	10. PROGRAM ELEMENT, PROJECT, TASK AREA & WORK UNIT NUMBERS
11. CONTROLLING OFFICE NAME AND ADDRESS: Department of the Interior, U.S. Geological Survey, Washington, DC 20242	12. REPORT DATE: Aug 1979
	13. NUMBER OF PAGES: 37
14. MONITORING AGENCY NAME & ADDRESS (if different from Controlling Office)	15. SECURITY CLASS. (of this report): UNCLASSIFIED
	15a. DECLASSIFICATION/DOWNGRADING SCHEDULE

16. DISTRIBUTION STATEMENT (of this Report)

Approved for public release; distribution unlimited.

17. DISTRIBUTION STATEMENT (of the abstract entered in Block 20, if different from Report)

18. SUPPLEMENTARY NOTES

DRCMS Code: 7-36AA-7100 HDL Project: A54735

This research is sponsored by the U.S. Geological Survey, Research and Development Program for OCS Oil and Gas Operations, under Technology Transfer Authorization.

19. KEY WORDS (Continue on reverse side if necessary and identify by block number)

Fluidics
Mud pulser
Down-hole telemetry
Measurement while drilling

20. ABSTRACT (Continue on reverse side if necessary and identify by block number)

Mud-pulse telemetry is a method for communicating diagnostic information from the bottom of a well to the surface while the well is being drilled. Because mud-pulse telemetry offers potential for improving the safety of hazardous offshore drilling operations, the U.S. Geological Survey has sponsored a research program at the Harry Diamond Laboratories (HDL) to investigate the

CONT

DD FORM 1 JAN 73 1473 EDITION OF 1 NOV 65 IS OBSOLETE

UNCLASSIFIED

SECURITY CLASSIFICATION OF THIS PAGE (When Data Entered)

163 050

20. Abstract (Cont'd)

CONT'

feasibility of applying fluidic flow control techniques to the design of a reliable high-speed pulser valve.

During these investigations, three subscale fluidic mud-pulsing circuits were tested over a wide range of drilling-fluid weights and viscosities to simulate well-bore conditions. The tests demonstrated that the unusual rheological properties of drilling mud cause only slight changes in circuit performance. Calculations of dynamic conditions in the drill string indicate that similar full-scale circuits would generate signal pressures of at least 37 psi (255 kPa) at a 200 gal/min (0.76 m^3/min) circulation rate.

Further tests of circuit dynamic response indicate that a similar full-scale pulser will have a frequency response of 15 to 20 Hz. Analytical investigations have shown that both signal amplitude and frequency response of these test circuits may be improved through design modifications.

HDL is now engaged in an ongoing effort to optimize the geometry of the subscale pulser circuit. A full-scale pulser will then be constructed and tested under surface and downhole conditions so that predicted performance can be verified.

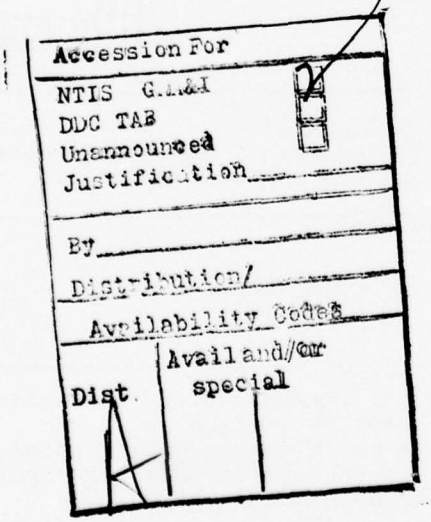

CONTENTS

FIGURES

TABLES

1. INTRODUCTION

Mud-pulse telemetry is a method for transmitting diagnostic information from the bottom of a well to the surface during normal drilling operations. This method has been under development for many years by the drilling industry because of the potentially great improvement that real-time downhole information can provide in drilling efficiency and safety. However, technological problems in pulser design have caused many delays in the application of the concept.

In a mud-pulse telemetry system, electrical signals from sensors near the drill bit are used to actuate a pulser valve. The valve responds by changing its effective port area, which in turn restricts the flow passing through the valve. Each time flow is restricted, a wave of increased pressure is produced through an effect commonly referred to as water hammer. The pressure waves travel through the mud column to the surface where they are detected by a pressure transducer. The sequence of waves is then decoded at the surface and displayed as measurements of downhole parameters for the driller.

Although this method is basically very simple and adaptable for use with conventional drill pipe hardware, the principal factor that has limited its use in the field is the availability of a reliable, high-speed pulser valve.

A mud-pulser valve must operate in severe well-bore environments of pressure, vibration, and shock. A valve of this type must also be designed to handle erosive fluids at flow rates comparable to full circulating rates. The harsh operating environments and physical loads on the valves severely limit the speed and reliability of the mechanical components in mud-pulser valves.

Because mud-pulse telemetry offers great potential for improved safety in offshore drilling operations, the Branch of Marine Oil and Gas Operations of the U.S. Geological Survey (USGS) has funded the U.S. Army's Harry Diamond Laboratories (HDL) to investigate the application of fluidic technology to mud-pulser valve design. Fluidic technology involves the use of fluid flow phenomena to perform control functions such as pressure amplification, digital logic, and flow throttling wihout moving parts. To perform these functions, fluidics uses only the energy contained in moving fluids and the interaction between these fluids and channels of fixed geometry. As an alternative to mechanical valving, fluidics allows higher operating speeds and increases reliability through the elimination of moving parts and seals.

The specific objectives of the fluidic mud-pulser program reported here were to

(a) determine changes in performance of fluidic components due to the unusual rheological properties of drilling muds,

(b) design fluidic circuits for pulsing mud flows,

(c) measure the performance of subscale circuits with drilling muds as test fluids,

(d) analyze circuit performance data to obtain guidelines for full-scale circuit design, and

(e) calculate dynamic conditions in the drill string so that performance of a full-scale pulser under downhole conditions can be predicted.

2. FLUIDIC PULSERS

2.1 General

Two fluidic components, a fluidic amplifier and a vortex valve, are employed in the mud-pulser valves described in this report. The components are used to control flow direction and rate in the valve. The essential features of each component are described in the following sections.

2.2 Fluidic Amplifier

A general proportional fluidic amplifier configuration is shown in figure 1. Typically, these devices contain a supply jet, one or more control jets, an interaction region, and one or more outlet ports. The channels are rectangular and usually formed by standard milling, chemical etching, or stamping.

Fluid passes through the supply nozzle in the form of a jet flow. Pressure recovered from the jet is available at the output. Control signals, consisting of pressures and flows smaller than those of the supply jet, impinge on the supply jet in the interaction region and deflect the supply jet between two outlets. This, in turn, alters the distribution of pressure across the outputs. Amplification occurs inasmuch as a change in output power in a particular outlet can be achieved with smaller changes in control power. The output may be proportional to the input signals (analog amplifiers, fig. 1) or respond bistably (digital amplifiers) to input commands.

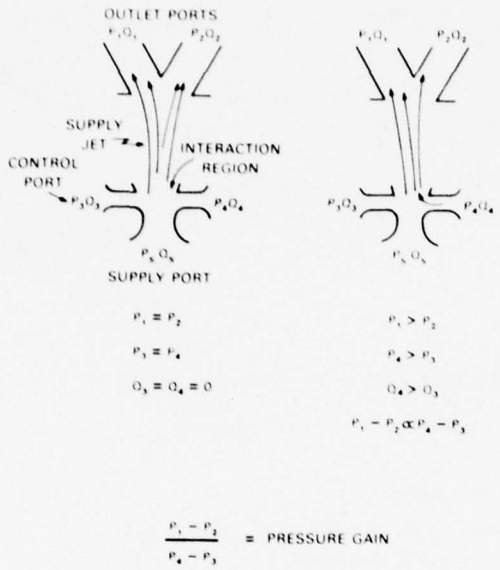

Figure 1. Proportional amplifier operation.

The flow geometry of a digital amplifier is shown in figure 2. In a digital device, each side of the supply jet is bounded by a wall imediately downstream from the control nozzles. The Coanda effect--a turbulent jet's property of attaching itself to a surface--causes the output of these devices to be bistable. This means only one of the outputs is pressurized at any given time. The output remains pressurized with or without a control input directing flow to that output port and regardless of output load. Flow switching occurs when pressure is applied to a particular control which is sufficient to force separation of the supply flow from the wall.

The gain (ratio of output power to control power) of a given device is determined by the relative location of the walls, the flow splitter, and the jet exhaust. Only a small deflection of the supply jet is required to initiate the full diversion of the supply jet to the opposite wall. This phenomenon is due to the viscous interaction (commonly called entrainment) between the high-velocity jet flow and the surrounding fluid. The proximity of the jet to the wall restricts the entrainment flow which, in turn, lowers the pressure between the jet and the wall that it is approaching. This action continues until the jet is sucked towards and finally attaches to the opposite wall. The location of the splitter with respect to the jet supply nozzle determines how much initial deflection must be caused by the control signal before this entrainment effect takes place.

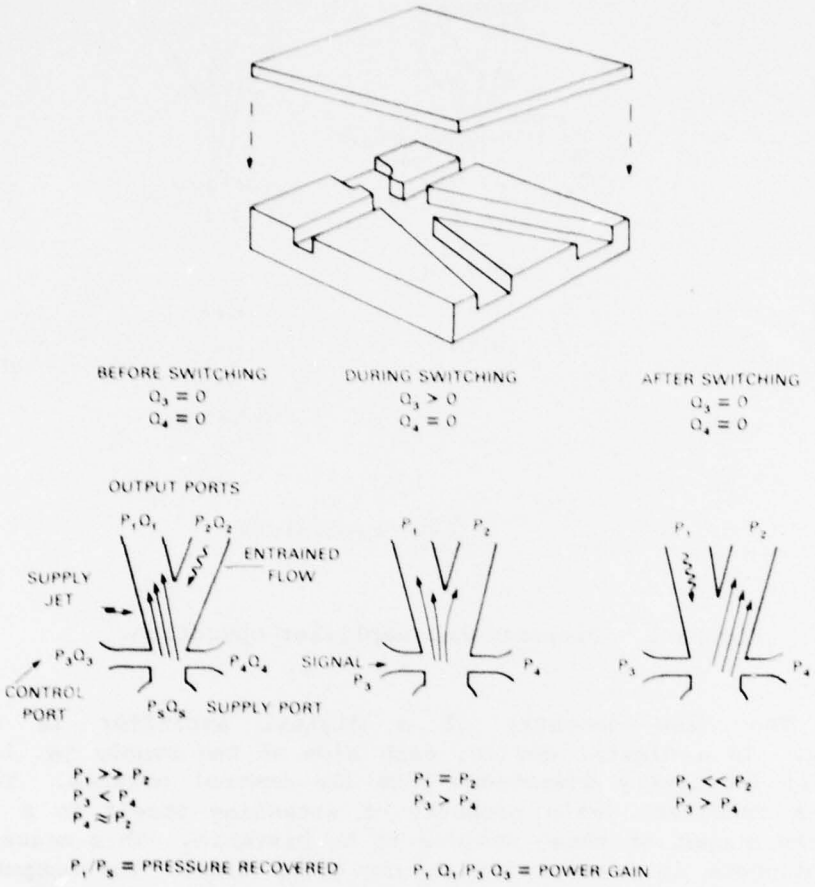

Figure 2. Bistable amplifier operation before, during, and after a control signal is applied.

The time required to direct the flow between outputs depends upon several geometric factors as well as the properties of the fluids. A detailed analysis of the factors governing response time is given by Drzewiecki.[1] Briefly, however, the time required for diverting the flow can be no shorter than the transport time for a particle of fluid to cover the distance between the supply nozzle and the outlet.

For amplifiers of this type, theory predicts and experiments verify[1] that the shortest response time is equal to approximately three times the transport time regardless of the magnitude of the control signal.

[1] *T. M. Drzewiecki, The Design of Flueric, Turbulent, Wall Attachment Flip-Flops, Proceedings of Fluidics State-of-the-Art Symposium, Vol. 1, Harry Diamond Laboratories (1972).*

2.3 Vortex Valve

The general arrangement of a vortex valve is shown in figure 3. The valve contains two inlet ports, an outlet port--referred to as a sink--and a cylindrical chamber. The sink nozzle has two effective outlet areas which are dependent upon which inlet is pressurized. When the radial inlet is pressurized, flow enters the chamber and travels directly to the sink, undergoing only the small pressure drop associated with entering a reservoir. The effective flow area of the sink is at its maximum value under this condition. When flow enters the chamber through the tangential inlet, a tangential velocity component is imparted to the flow by the chamber walls, and a large pressure drop is developed across the valve because of the centrifugal forces exerted by the rotating fluid. The increased resistance or reduction in effective area reduces the amount of flow which can pass through the valve.

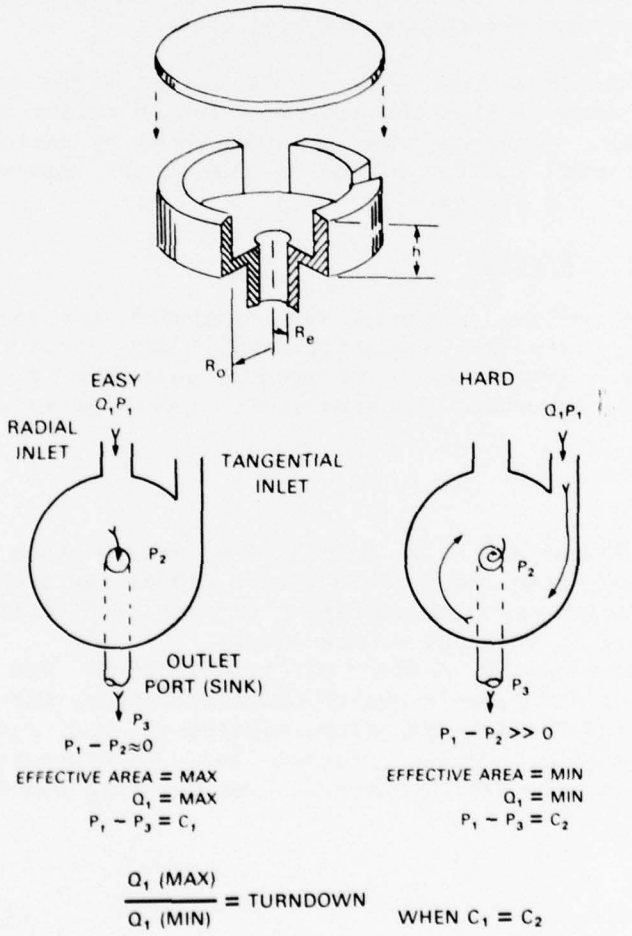

Figure 3. Vortex valve operation showing easy and hard flow directions.

With a constant pressure drop across the valve, the ratio between the maximum flow and minimum flow which can be passed through the valve in each case is used to define the change in effective port area. This ratio, referred to as turndown, is used to indicate the valving effectiveness of the device. In this report the turndown ratio is obtained from measurements of each flow rate at equal pressures between the inlet ports and the pressure at the sink nozzle exhaust. The geometric parameters which influence turndown include normalized radius, r_o/r_e, and normalized depth, h/r_e, where r_o is chamber radius, r_e is exhaust nozzle radius, and h is chamber depth.

A great deal of research and development work has been devoted to the study of vortex devices of various types. Results of many of these studies are summarized elsewhere.[2-4] Much of this work was directed towards optimizing turndown and frequency response. Turndown ratios of 3 to 10 are considered typical. Since the effective port area of a given device determines flow capacity and other physical dimensions, it also determines response time.

The response time of a vortex valve is the time required for the effective area or flow through the valve to change from a maximum to a minimum level. Response time has been shown by various experimenters to be proportional to the volume of the vortex chamber and inversely proportional to the flowrate.

2.4 Pulser Circuits

Three pulser circuits were designed and tested during the course of the mud-pulser investigations. Each circuit uses a fluidic amplifier and a vortex valve to produce effective flow area changes. Each circuit is described in terms of its operation as a mud pulser.

---

[2] *B. E. A. Jacobs and P. J. Baker, The Steady-State and Transient Performance of Some Large Scale Vortex Diodes, British Hydromechanics Research Association, Proceedings of the 5th Cranfield Fluidics Symposium, Vol. 1, Uppsala, Sweden (1972).*

[3] *D. N. Wormley, A Review of Vortex Diode and Triode Static Characteristics and Dynamic Design Characteristics, MIT Proceedings of Fluidic State-of-the-Art Symposium, Washington, D.C. (1974).*

[4] *S. S. Fineblum, Vortex Diodes, Bell Laboratories Proceedings, Fluidic State-of-the-Art Symposium, Vol 1, Harry Diamond Laboratories (1974).*

2.5 Circuit A

Figure 4A describes the essential operating features and general flow configuration of circuit A. In figure 4A the amplifier jet is shown attached to the wall leading to the radial inlet of the vortex valve (solid arrows). Since the flow passes directly to the sink, the resulting pressure drop across the circuit is low. To switch the pulser from this easy-flow state to one in which the flow rate is reduced (the hard-flow state), a control signal in the form of a short-duration pressure pulse is introduced through control port 1.

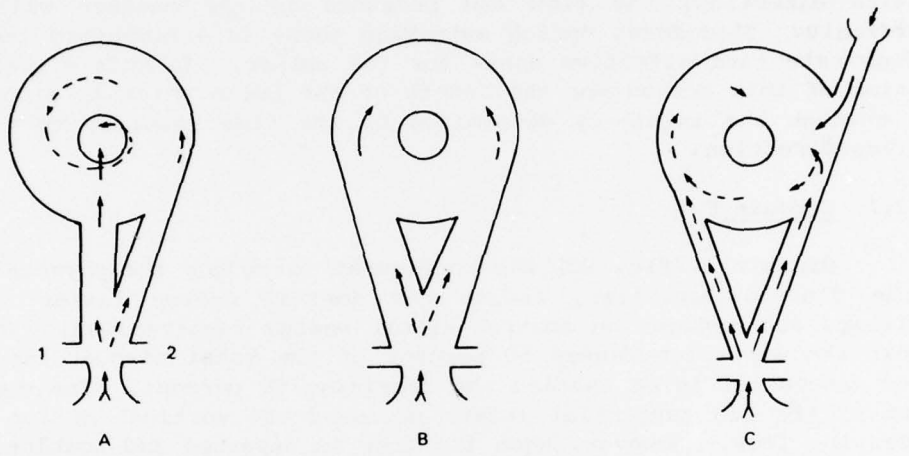

Figure 4. Pulser geometries for circuits A, B, and C.

As the control pulse exits the control nozzle, the energy (pressure times flow) in the pulse raises the pressure between the supply jet and the wall. The rise in pressure separates the attached flow from the wall and causes the jet to attach to the opposite wall, as shown by the broken arrows. The energy associated with the supply jet flow produces a vortex which reduces the effective area of the sink nozzle. As the flow area is reduced, the pressure in the radial port increases and reduces the amount of flow which can pass through the amplifier and drill string. The energy of the inlet flow is then expended in compressing the flow entering the valve. A wave (water hammer) of increased pressure forms and propagates back through the string. The pressure is returned to its original level when the jet is deflected by a second control pulse (through port 2) back to its former state. The change in pressure produced by the change in effective flow area or inlet velocity represents the signal which would carry digitized information to the surface.

2.6 Circuit B

The operation of circuit B (fig. 4B) is similar to that of circuit A with one exception: the amplifier supply jet is used to alternately pressurize one of two tangential inlets to the vortex chamber. In either stable state, the flow through the pulser is restricted. However, the direction of the rotating flow is reversed each time a signal is applied across the controls. Since the flow rate or pressure drop in the vortex chamber depends on the tangential velocity of rotation and since the tangential velocity goes from a maximum value in one direction through zero to a maximum value in the opposite direction, the flow and pressure in the chamber will vary accordingly. Therefore, during switching there is a momentary increase in flow rate (and effective area) for the pulser. In this circuit the duration of this action--or the length of the pulse which is propagated back through the inlet--is determined by the time required to reverse the flow direction.

2.7 Circuit C

Circuit C (fig. 4C) was configured to reduce the physical size of the fluidic amplifier, reduce the nominal energy losses in the amplifier, and reduce the control-signal energy requirements. In this circuit the amplifier passes 50 percent of the total circuit flow; the second tangential inlet carries the remaining 50 percent. The combined effect of the two tangential inlets produces the vortical motion which impedes the flow. However, when the flow is diverted and combines with the flow issuing through the second inlet, the vortex ceases, and the valve discharges flow easily. The flow remains in this condition until a control pulse is applied, and the action is reversed.

2.8 Mud-Pulser Circuit Analysis

The performance of a fluidic mud pulser has been analyzed in terms of the flow and pressure conditions in the pulser. This analysis allows for both greater understanding of the loss mechanisms in the pulser and easy comparison of the performance of various pulser models. Losses in the pulser are especially detrimental in the easy flow direction because they not only tend to decrease the turndown ratio but also require a larger pulser to pass the required flow at a given pressure drop.

Losses in a pulser result from loss of dynamic head through friction. These losses occur between the power jet of the fluidic amplifier and the exit nozzle of the vortex valve. The average power jet velocity (V_{pj}) is found from the flow rate (Q) through the pulser.

$$V_{pj} = \frac{Q}{A_1} \quad , \tag{1}$$

where A_1 is the area of the power jet.

The velocity head of the power jet is the pressure drop from the total pressure (P_o) feeding the amplifier to the static pressure (P_i) in the amplifier. Thus

$$P_o - P_i = \frac{1}{2} \rho \left(\frac{V_{pj}}{k_1} \right)^2 \quad , \tag{2}$$

where ρ is the density of the fluid passing through the pulser, and k_1 is the discharge coefficient. A portion of this kinetic energy is lost to turbulence and friction while the fluid passes through the amplifier, and another portion is lost when the fluid enters the vortex valve chamber. If the pressure recoverable in the output leg of the amplifier is $R_1(P_o - P_i)$, where R_1 is an assumed pressure recovery factor, then the total pressure recovered in the vortex valve is $P_i + R_1R_2(P_o - P_i)$, where R_2 is the fraction of the remaining kinetic energy recovered in the vortex valve. The flow rate through the vortex valve is thus

$$Q = A_2 k_2 \sqrt{2\left[P_i + R_1R_2 \left(P_o - P_i\right) - P_B\right]/\rho} \quad , \tag{3}$$

where A_2 is the area of the vortex valve outlet, k_2 is the associated discharge coefficient, and P_B is the back pressure on the vortex valve. Equation (2) may be used to eliminate P_i so that

$$Q = A_2 k_2 \sqrt{2\left[P_o - P_B - \left(1 - R_1R_2\right) \frac{\rho}{2} \left(\frac{V_{pj}}{k_1} \right)^2 \right]/\rho} \quad . \tag{4}$$

Equation (4) may be written completely in terms of measured parameters by use of equation (1). Solving for the vortex valve discharge coefficient, k_2, yields

$$k_2 = Q/A_2 \sqrt{\left[2\left(P_o - P_B\right)/\rho\right] - \left(1 - R_1R_2\right)Q^2/A_1^2K_1^2} \quad . \tag{5}$$

Equation (5) has been used in the analysis of experimental data taken on mud-pulser circuit A. The experiment and analysis are described in section 3.2.

The effective area, A_{eff}, of a pulser is defined as that area which, when subjected to the same pressure differential as the circuit, passes the same flow rate. The effective area is, thus, given by

$$A_{eff} = Q/\sqrt{2\left(P_o - P_B\right)/\rho} \quad . \tag{6}$$

Equation (6) can be used to calculate the effective area of a pulser circuit from experimentally determined values of flow rate and pressure drop.

By solving equation (5) for Q and combining it with equation (6), we can show that the effective area is given by

$$1/A^2_{eff} = \left[\left(1 - R_1 R_2\right)/A^2_1 k^2_1\right] + 1/A^2_2 k^2_2 \quad . \tag{7}$$

Therefore, once discharge coefficients are known for the fluidic amplifier nozzle and the vortex valve exhaust nozzle, equation (7) may be used to estimate changes in a circuit's effective area as improvements are made in pressure recovery or discharge coefficient.

3. EXPERIMENTS AND RESULTS

3.1 Introduction

An experimental investigation of pulser circuits A, B, and C has been conducted to (a) determine the performance changes in specific pulser test circuits when drilling muds are employed as the flow media, (b) relate changes in performance to changes in properties, (c) establish a method of estimating the type of performance which current circuit configurations would provide in a full-scale circulating system, and (d) estimate how possible design improvements might affect the overall functional characteristics of a fluidic mud-pulse telemetry transmitter.

The principal experiments were conducted on circuit A. These experiments consisted of measuring the pressure-flow characteristics of circuit A in the easy flow and restricted (hard) flow operating modes.

Additional experiments were conducted on circuits A, B, and C to verify amplifier bistability, to measure frequency response, and to provide qualitative information on flow modulation and overall performance.

The test circuits used in the experiments were formed in flat brass base plates by the use of an optical tracer milling machine. The base plate contained all flow channels. The channels were covered with a second plate which was secured with screws and contained pressure taps and control input connectors. Figure 5 shows the circuit A assembly.

The test fluids were formulated with water as the base fluid, bentonite to build viscosity, and barite as a weighting material. Table I lists properties of the three muds used to test the pulser (water was also used as a test fluid). Mud I was made from fresh water with 20 lb/barrel* of bentonite. Mud I was an unweighted mud with a density of 8.4 ppg (pounds per gallon).† Mud II was made from Mud I by weighting it up with barite to a density of 12.0 ppg. Mud II was then diluted with water and weighted up with barite to a density of 15.3 ppg to make Mud III. Mud rheological properties were measured with a Baroid variable-speed viscometer. The gel strength and yield point are considered quite high for Mud III, while its plastic viscosity and density have moderate to high values for drilling muds found in the field.

TABLE I. MUD PROPERTIES

Property	Mud I	Mud II	Mud III
Density (ppg)[a]	8.4	12	15.3
Plastic viscosity (cps)[b]	11	20	27
Yield point ($lb/100\ ft^2$)[c]	8	19	6
Gel strength ($lb/100\ ft^2$)			
10 s	7	30	23
10 min	28	85	51

[a] $(ppg)119.8 = (kg/m^3)$

[b] $(cps)10^{-3} = (Pa \cdot s)$

[c] $(lb/100\ ft^2)0.4788 = (Pa)$

*$(lb/barrel) = \sim(g/350\ cm^3)$.

†$(ppg)119.8 = (kg/m^3)$.

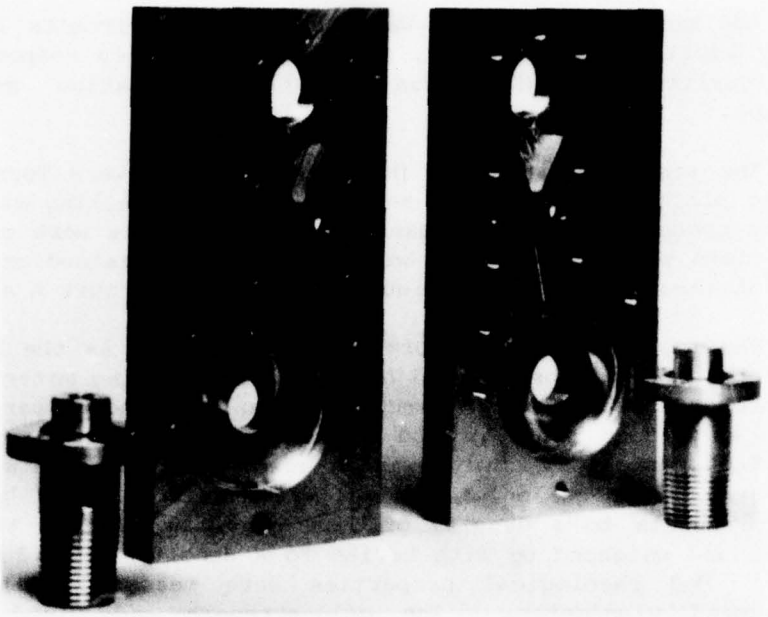

Figure 5. Circuit A assembly.

The test apparatus used for the circuit A experiments is shown schematically in figure 6. High-pressure nitrogen was used to circulate mud from the supply chamber through a second chamber containing the test circuit and into a reservoir chamber. The operating pressure across the test circuit was maintained by a supply regulator and a back-pressure regulator located on the top of each container.

A back pressure of 200 psi* was maintained during all tests to eliminate cavitation in the circuit. This back pressure was considered high enough to eliminate cavitation for supply pressures up to 400 psi (200-psi differential pressure across the pulser). Higher back pressures were not considered necessary even though downhole well-bore pressures reach 10,000 psi or greater, because fluid properties (viscosity and density) do not change significantly even at these high pressures. Test fluid viscosities and densities varied over much wider ranges than back pressure can cause, so the tests are considered representative of downhole conditions.

*(psi)6.895 = (kPa).

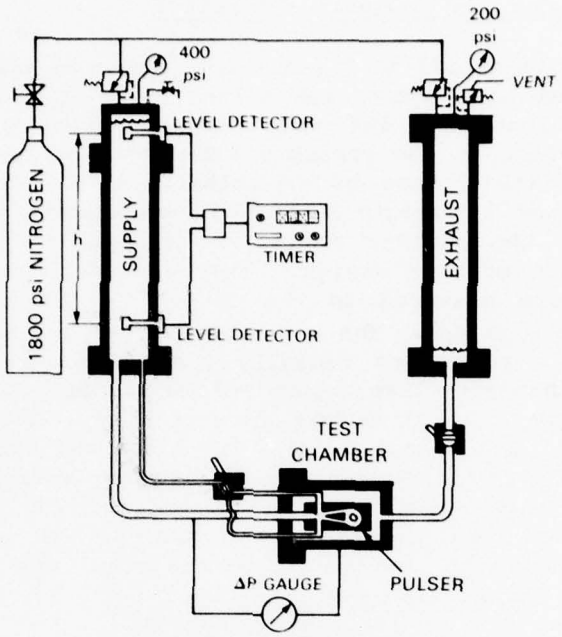

PULSER FLOW DIAGRAM

(psi) 6.895 = (kPa)

Figure 6. Test apparatus for circuit A.

The direction of flow through the test circuit (hard or easy flow state) was set during circulation but before flow measurements were made. The direction was set by allowing a pressurized flow to enter the required control port through a three-way valve. The control flow was then shut off while flow measurements were made.

The flow rate was determined from measurements of the time required to displace a known volume of fluid. Two ultrasonic level detectors located a fixed distance apart were used to actuate a timer. The distance between the detectors and the cross-sectional area of the chamber determined the supply volume, which was measured to be 3.01 gal.*

*(gal)3.785 × 10^{-3} = (m^3).

3.2 Test Results and Analysis--Circuit A

From equations (1) to (6) and from measured values of flow rate (Q) versus pressure drop across the pulser $(P_o - P_B)$, it is possible to calculate jet velocities, internal static pressures (P_i), and the discharge coefficient of the vortex valve--provided certain assumptions are made about dynamic losses in the pulser. In the following analysis of the data obtained on circuit A, it has been assumed that the pressure recovery (R_1) of the fluidic amplifier is 0.5, a typical value for bistable amplifiers of this design. This assumption means that if the total pressure were measured in the output leg of the amplifier, it would be $P_i + 0.5(P_o - P_i)$. The jet from the output leg then enters the vortex valve. If it enters radially (the easy direction), then the vortex valve chamber acts like a pure volume and all the dynamic head is lost to turbulence. If it enters tangentially (the hard direction), then, ideally, all the energy in the jet forms the vortex, and none of the dynamic head is lost. Thus, in the following analysis of mud-pulser performance data, the pressure recovery (R_2) of the vortex valve has been assumed to be zero in the easy direction and unity in the hard direction. The discharge coefficient of the fluid amplifier was assumed to be 0.95 in all calculations.

The most significant measure of pulser performance is its effective area, A_{eff}, defined in equation (6). It is this effective area that changes when the pulser switches between its easy and hard flow directions. The ratio (at a constant pressure drop across the pulser) of the effective area in the easy direction to the effective area in the hard direction is defined as the turndown ratio of the mud-pulser circuit.

The effective areas calculated from the data taken on pulser circuit A are presented in figure 7. This circuit had an amplifier power jet area of 0.04 $in.^2$* (0.4-in. depth, 0.1-in. width) and a vortex valve outlet area of 0.0556 $in.^2$ (0.266-in. diameter). Turndown ratios derived from these data are 2.7 for water, 2.45 for Mud I, and 2.35 for Muds II and III.

It is interesting to note that the effective area increases in both the easy and hard directions as the mud viscosity increases. In the easy direction, this increase is probably due to decreased turbulence in the vortex valve chamber; in the hard direction, the increase is probably due to increased radial leakage to the drain through the boundary layer of the vortex.

Maximum power jet velocities (neglecting losses) through the fluid amplifier are shown in figure 8 as a function of pressure drop across the pulser. These velocities were calculated from the data taken

*(in.)2.54 = (cm).

on the pulser and the dynamic head calculated from equations (1) and (2). These jet velocities are the highest velocities in the pulser and should be used for erosion considerations.

The vortex valve discharge coefficient (again calculated from data taken on the pulser) is shown in figure 9 as a function of pressure drop across the vortex valve. The coefficient in the easy direction varies from about 0.45 to 0.7. This low value indicates the possibility of some vorticity in the flow pattern in the vortex chamber even in the easy direction. Eliminating this vorticity could significantly improve the pulser performance--provided the fluidic amplifier could also be increased in size to keep the power jet velocities low. As shown in section 4, however, even the turndown ratios achieved with circuit A are sufficient for generating high-amplitude signal pressures in the mud flow. Further improvement of pulser efficiency, however, would allow greater design flexibility.

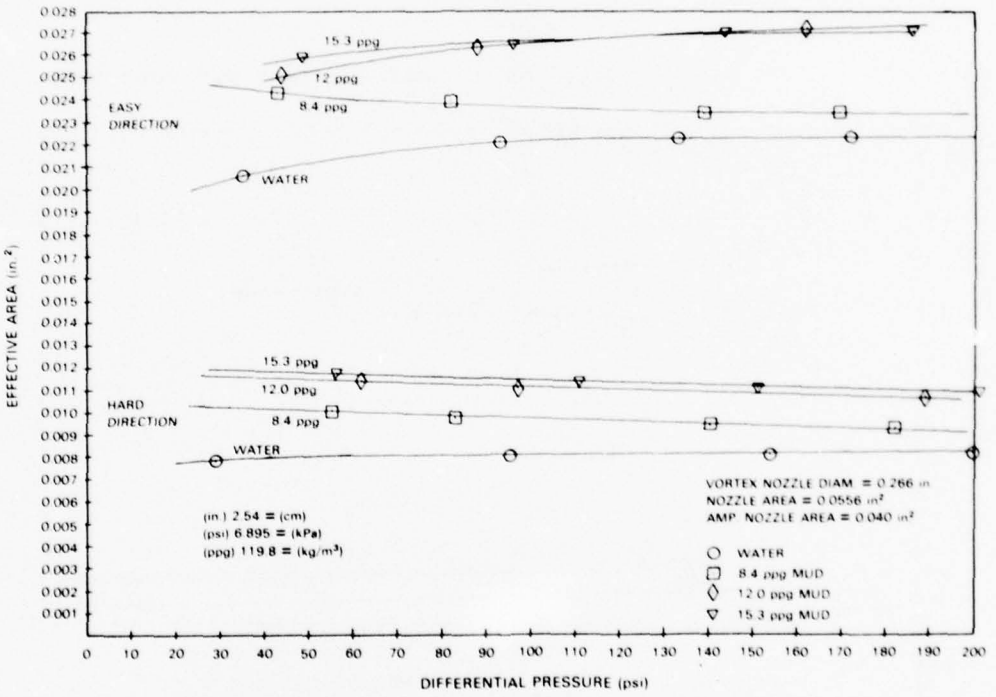

Figure 7. Effective area of circuit A versus pressure drop.

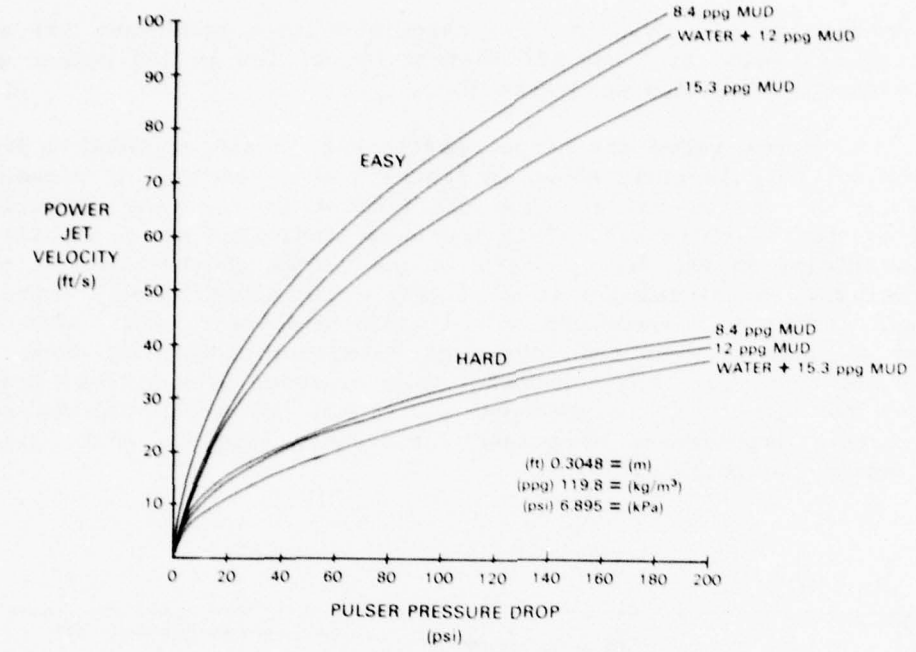

Figure 8. Power jet velocity for circuit A versus pressure drop.

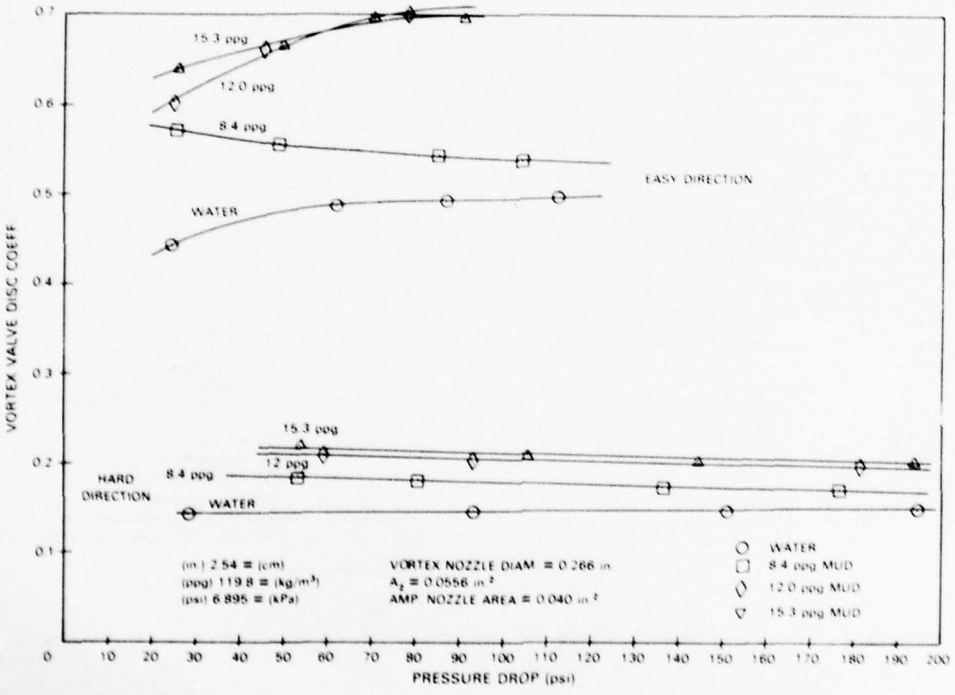

Figure 9. Vortex valve discharge coefficient versus pressure drop.

3.3 Mud-Pulser Flow Tests--Circuits B and C

The flow tests on circuit A showed that pulser performance could be significantly improved if the discharge coefficient of the vortex valve in the easy flow direction could be improved. Circuits B and C were designed to achieve this improvement.

In circuit B, the easy flow direction is not a stable state but exists only as the transition between the two states of high vorticity in opposite directions. Thus, the turndown ratio could not be directly measured. An experiment is currently under design to measure the turndown indirectly as a function of pressure drop across the pulser. Circuit B was operated with tap water at about 30-psi power jet pressure while high-speed movies were taken of the vortex valve exhaust flow. The movies showed that a jet of well-streamlined flow left the vortex valve between stable states of high vorticity. Figure 10 is a sample film strip. The sequential photographs illustrate the change in flow pattern at the exhaust nozzle of the pulser as it switches. The parallel streamlines indicate maximum flow from the pulser; the umbrella-shaped streamlines illustrate the high vorticity of the minimum flow condition.

In further tests on circuit B, the static pressure in the output leg of the fluidic amplifier was monitored with a piezoelectric pressure transducer. The pulser was supplied directly from a pressurized reservoir at pressures up to 60 psi. The supply pressure was thus constant during switching of the pulser; however, the static pressure in the output leg of the amplifier dropped significantly during switching because of the temporary increase in vortex valve effective area. It was not possible with the equipment used to obtain quantitative measurements of pressure amplitudes, but the duration of the pressure drop was determined. In this case the duration of the pressure drop indicates the period of the maximum operating frequency of the vortex valve.

The measurements showed that, for the subscale pulser tested, the period of switching is inversely proportional to flow rate (or the square root of the pressure drop) through the pulser. At 60-psi pressure drop across the pulser, the period was about 30 ms, corresponding to a frequency of 33 Hz. Tests with Mud III showed no difference in response time between mud and water.

Theory indicates that the response time of a vortex valve is inversely proportional to flow rate but directly proportional to the volume of the vortex chamber. This means that, when the present pulser is scaled up to a full-size operating valve, the response time will be proportional to the linear scaling factor. Present estimates are that a

full-scale (400 gal/min) pulser operating at a pressure differential of 100 psi or greater will have an upper cutoff frequency between 15 and 20 Hz. This should be considered a minimum estimate of cutoff frequency, because further improvements in valve dynamics can be expected.

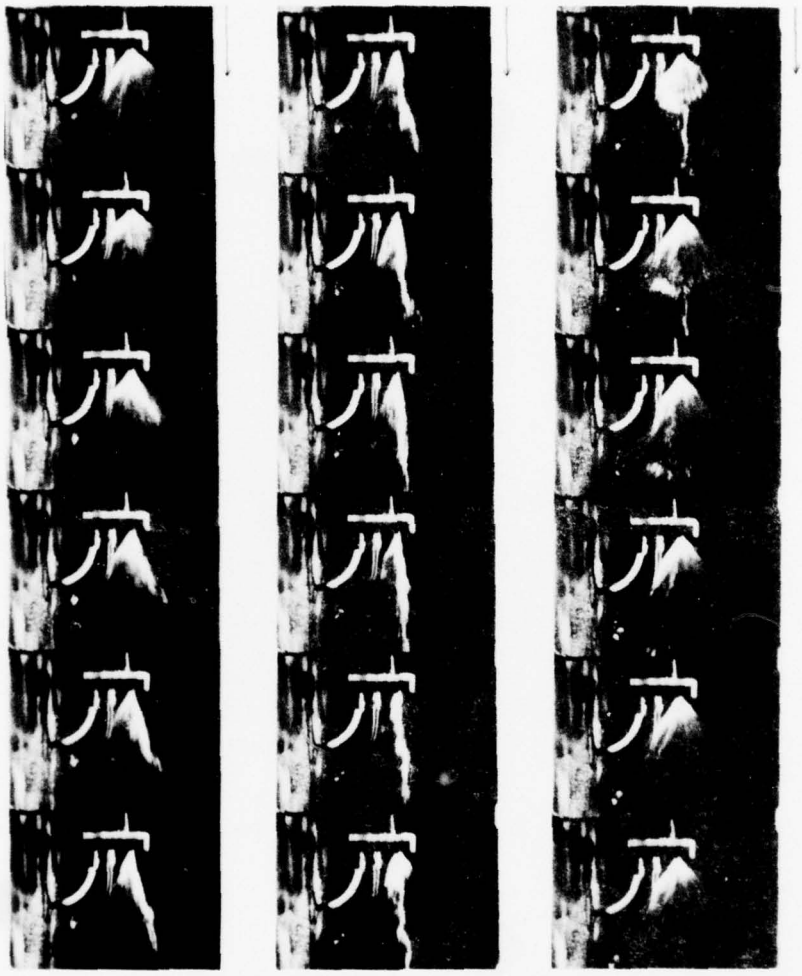

Figure 10. Sequential photographs of the switching of circuit B (200 frames/s).

Circuit C is a modification of circuit B to provide a stable easy flow condition. Only brief qualitative observations have been made to date on circuit C with tap water at low pressure differentials. These tests established that flows from the two inlets into the vortex valve could be balanced to provide a stable easy flow condition. Although no measurements were made, switching of the pulser appeared as rapid as for circuits A and B.

4. ANALYSIS OF DYNAMIC PERFORMANCE IN A CIRCULATING SYSTEM

To predict the dynamic performance of a mud pulser in a circulating system, it is necessary to account for the dynamic flow conditions in the drill string as well as the performance of the pulser. If, for example, the pulser is close to the mud pump, the steady-state flow conditions will be attained quickly even if the effective area of the pulser is changed rapidly. Under steady flow conditions, the pressure drop across the valve will be inversely proportional to the square of the effective area of the pulser, because the flow rate will remain virtually constant even though the effective area of the valve has changed.

If, however, the pulser were situated downhole, a change in pressure at the pulser (caused by a change in pulser area) would not be sensed at the pump until the pulse traveled the distance between the pulser and pump at the speed of sound. Thus, by the time the mud pump is affected by the initial change in area, the pulser will have changed area many times. Under these conditions the flow rate through the pulser will not remain constant. For this case, the pressure signal generated by the pulser as its effective area is changed will be determined by the water-hammer relationship between the change in flow and the change in pressure.

The time-averaged flow rate through the pulser is determined by the pumping rate set at the surface. If the pulser is assumed to have two states with effective areas $A1_{eff}$ and $A2_{eff}$, then there will be two flow rates, Q_1 and Q_2, in the drill pipe at the pulser. If it is additionally assumed that the pulser spends equal times in these two states, then the average flow rate is $(Q_1 + Q_2)/2$. Thus, if the pump rate is Q, then

$$Q_1 + Q_2 = 2Q \quad . \tag{8}$$

The water-hammer relationship determines the relationship between the change in flow rate and the change in pressure upstream of the pulser; thus,

$$Q_1 - Q_2 = K(P_2 - P_1) \quad , \tag{9}$$

where $K = A/\rho C$, A is the internal area of the pipe, ρ is the density of the fluid passing through the pulser, C is the speed of sound in the fluid, and P_1 and P_2 are the pressure upstream of the pulser for the two pulser states. If the pulser is assumed to be in series with and upstream of a drill bit with an effective area A_3, then the following equations relate the flow rate to the pressure drop across the pulser and the drill bit (pressure downstream of the drill bit is assumed constant and all presures are referenced to it):

$$Q_1^2 = K_1^2 \left(P_1 - P_{B1}\right) \quad , \tag{10}$$

$$Q_1^2 = K_2^2 \left(P_2 - P_{B2}\right) \quad , \tag{11}$$

$$Q_1^2 = K_3^2 \left(P_{B1}\right) \quad , \tag{12}$$

$$Q_2^2 = K_3^2 \left(P_{B2}\right) \quad , \tag{13}$$

where, for the two pulser states, P_{B1} and P_{B2} are the pressures between the pulser and the bit, $K_1 = A1_{eff}\sqrt{2/\rho}$, $K_2 = A2_{eff}\sqrt{2/\rho}$, and $K_3 = A3\sqrt{2/\rho}$. These six equations--(8) through (13)--have six unknowns, Q_1, Q_2, P_1, P_2, P_{B1}, and P_{B2}, so they uniquely describe the operating conditions at the pulser when the pulser effective areas, $A1_{eff}$ and $A2_{eff}$, the bit effective area, A_3, and the average flow rate, Q, are given.

Equations (8) through (13), when solved for Q_2, result in the following quadratic equation in Q_2.

$$Q_2^2 \left(\frac{1}{K_{23}^2} - \frac{1}{K_{13}^2}\right) + Q_2\left(\frac{2}{K} + \frac{4Q}{K_{13}^2}\right) - \left(\frac{4Q^2}{K_{13}^2} + \frac{2Q}{K}\right) = 0 \quad , \tag{14}$$

where

$$1/K_{13}^2 = \left(1/K_1^2\right) + \left(1/K_3^2\right)$$

and

$$1/K_{23}^2 = \left(1/K_2^2\right) + \left(1/K_3^2\right)$$

If we define

$$a = \frac{1}{K_{23}^2} - \frac{1}{K_{13}^2} ,$$

$$b = \frac{2}{K} + \frac{4Q}{K_{13}^2} , \quad \text{and}$$

$$c = -\left(\frac{4Q}{K_{13}^2}\right) + \frac{2Q}{K}$$

then Q_2 is given by

$$Q_2 = \frac{-b + \sqrt{b^2 - 4ac}}{2a} \tag{15}$$

From equations (8) through (13), the following relationships can be found.

$$Q_1 = 2Q - Q_2 \tag{16}$$

$$P_{B1} = Q_1^2/K_3^2 \tag{17}$$

$$P_{B2} = Q_2^2/K_{32}^2 \tag{18}$$

$$P_1 = Q_1^2/K_{13}^2 \tag{19}$$

$$P_2 = Q_2^2/K_{23}^2 \tag{20}$$

Thus, given the effective areas of the mud pulser (A_1 and A_2), the bit area (A_3), the mud density (ρ), and the average flow rate through the pulser (determined by the flow rate (Q) at the pump), it is possible to calculate the dynamic downhole conditions. The results of such a calculation are shown in table II along with calculations of the steady-state pressure that would be expected if the pulser were closer to the mud pump or if it were steadily operated in either the easy or hard direction. The relationships in table II apply to any mud pulser in which the area changes are as indicated.

TABLE II. PULSER DYNAMIC PERFORMANCE

Drill pipe ID = 3.75 in. (9.52 cm)
Bit area = 0.35 in.^{2} (2.26 cm^2)
Mud density = 10 ppg (1198 kg/m^3)
Sound speed = 4710 ft/s (1435 m/s)
Easy pulser area, $A1_{eff}$ = 1.0 in.^{2} (6.45 cm^2)

Average circulation flow rate (gal/min),[a]	Pulser operating conditions[b]										
	Steady state				Dynamic						
	Bit pressure (psi)[c]	Upstream pressure (psi)[c]		Signal pressure (psi)[c]	Flow rate (gal/min)[a]		Bit pressure (psi)[c]		Upstream pressure (psi)[c]		Signal pressure (psi)[c]
		Hard	Easy		Hard	Easy	Hard	Easy	Hard	Easy	
For flow rate = 100	75	108	83	25	97	103	70	79	102	88	14
200	299	432	332	100	192	208	275	324	397	360	37
400	1197	1728	1329	401	380	420	1078	1321	1557	1468	89
$A2_{eff}$ = 0.5 in.^{2} (3.2 cm^2) (Turndown = 2)											
For flow rate = 100	75	208	83	125	88	112	57	94	159	105	54
200	299	831	332	499	168	232	211	402	587	447	140
400	1197	3322	1329	1993	325	475	792	1684	2200	1871	329
$A2_{eff}$ = 0.25 in.^{2} (1.6 cm^2) (Turndown = 4)											

[a] (ft/s)0.3048 = (m/s)

[b] All pressures are referenced to downhnhole pressure

[c] (psi)6.895 = (kPa)

Examination of table II shows that the dynamic signal pressure (water hammer) is much less than would be expected from steady-state operating characteristics. However, if the turndown ratio is greater than 2 and the flow rate is 200 gal/min* or higher, then the dynamic signal pressure is at least 37 psi.

Use of calculations such as these allows pulser size and turndown ratios to be optimized for a given bit area and mud flow rate. Accurate calculations of downhole conditions are also necessary for valid interpretation of field-test data.

*(gal/min)$6.31 \times 10^{-5} = m^3/s$.

5. SUMMARY AND CONCLUSIONS

The HDL mud-pulser program is being conducted to determine areas in which fluidic technology can be applied for the improvement of mud-pulser valve speed and reliability. To date the program has consisted of an experimental and analytical study of three subscale fluidic mud-pulsing circuits. The results of the study are as follows.

(1) The unusual rheological properties of drilling mud do not significantly affect the bistable operation of digital fluidic amplifiers for the scale and flow rate of the tests.

(2) The increased viscosity of drilling mud causes a slight increase (relative to water) in the effective area of the vortex valve in both the maximum and minimum flow states.

(3) The turndown ratio of the experimental pulser circuit A varied from 2.7 for water to 2.35 for 15.3 ppg mud.

(4) The pulser turndown ratio can be improved over the experimental model by an increase in the vortex valve discharge coefficient in the maximum flow state.

(5) Measured response times for circuit B indicate that a full-scale pulser valve will have a frequency response of 15 to 20 Hz. This response could possibly be increased through improved valve dynamics.

(6) Calculations of dynamic conditions in the drill string indicate that the turndown ratios of the experimental pulser would generate signal pressures of at least 37 psi at a 200-gal/min circulation rate.

HDL is now engaged in an ongoing effort to optimize the geometry of the subscale pulser circuit for turndown ratio and frequency response. A full-scale pulser will then be constructed and tested under surface and downhole conditions so that predicted performance can be verified.

NOMENCLATURE

A	Drill pipe internal area
A_{eff}	Effective areas of the mud-pulser valve, defined in equation (6)
A_1	Power jet area for the bistable amplifier
$A1_{eff}$	One of the two pulser effective areas
A_2	Area of the vortex valve outlet
$A2_{eff}$	One of the two pulser effective areas
A_3	Total bit nozzle effective area
a	Coefficient of quadratic equation
b	Coefficient of quadratic equation
C	Speed of sound
c	Coefficient of quadratic equation
h	Depth of vortex valve chamber
K	Water-hammer equation coefficient
K_1	Defined in text, equation (10)
K_2	Defined in text, equation (11)
K_3	Defined in text, equation (12)
K_{13}	Defined in text, equation (14)
K_{23}	Defined in text, equation (14)
k_1	Discharge coefficient for the bistable amplifier
k_2	Discharge coefficient for the vortex valve exhaust nozzle
P_B	Pressure downstream of the vortex valve
P_{B1}	One of the two drill-bit pressures during pulser operation (pulser effective area = $A1_{eff}$)
P_{B2}	One of the two drill-bit pressures during pulser operation (pulser effective area = $A2_{eff}$)

NOMENCLATURE (Cont'd)

P_i	Internal static pressure in the bistable amplifier
P_o	Total pressure supplied to the mud pulser
P_1	One of the two pressures upstream of the pulser during operation (pulser effective area = $A1_{eff}$)
P_2	One of the two pressures upstream of the pulser during operation (pulser effective area = $A2_{eff}$)
Q	Average flow rate through the pulser
Q_1	One of the two flow rates through the pulser during operation (pulser effective area = $A1_{eff}$)
Q_2	One of the two flow rates through the pulser during operation (pulser effective area = $A2_{eff}$)
R_1	Pressure recovery of the bistable amplifier
R_2	Pressure recovery in the vortex valve
r_e	Vortex valve exhaust nozzle radius
r_o	Vortex valve chamber radius
V_{pj}	Bistable amplifier power jet velocity
ρ	Fluid density

DISTRIBUTION

COMMANDER IDDR&E
PENTAGON, ROOM 3D 1089
WASHINGTON, DC 20310
ATTN LTC G. KOPESAK

DEFENSE DOCUMENTATION CENTER
CAMERON STATION, BUILDING 5
ALEXANDRIA, VA 22314
ATTN DDC-TCA (12 COPIES)

COMMANDER
US ARMY RSCH & STD GP (EUR)
ATTN LTC JAMES M. KENNEDY, JR.
CHIEF, PHYSICS & MATH BRANCH
EPO NEW YORK 09510

COMMANDER
US ARMY MATERIEL DEVELOPMENT &
READINESS COMMAND
ATTN DRXAM-TL, HQ TECH LIBRARY
5001 EISENHOWER AVENUE
ALEXANDRIA, VA 22333

COMMANDER
US ARMY MISSILE & MUNITIONS
CENTER & SCHOOL
ATTN ATSK-CTD-F
REDSTONE ARSENAL, AL 35809

DIRECTOR
US ARMY MATERIEL SYSTEMS
ANALYSIS ACTIVITY
ATTN DRXSY-MP
ABERDEEN PROVING GROUND, MD 21005

DIRECTOR
US ARMY BALLISTIC RESEARCH LABORATORY
ATTN DRDAR-TSB-S (STINFO)
ABERDEEN PROVING GROUND, MD 21005

TELEDYNE BROWN ENGINEERING
CUMMINGS RESEARCH PARK
ATTN DR. MELVIN L. PRICE, MS-44
HUNTSVILLE, AL 35807

CONSERVATION DIVISION
US GEOLOGICAL SURVEY
12201 SUNRISE VALLEY DRIVE
RESTON, VA 22070
ATTN JOHN GREGORY (50 COPIES)

OFFICE OF THE DEPUTY CHIEF OF STAFF
FOR RESEARCH, DEVELOPMENT &
ACQUISITION
DEPARTMENT OF THE ARMY
WASHINGTON, DC 20310
ATTN DAMA-ARP-P, DR. V. GARBER
ATTN MR. JOHN HILL, ROOM 3D424

US ARMY R&D GROUP (EUROPE)
BOX 15
FPO NEW YORK 09510
ATTN CHIEF, AERONAUTICS BRANCH
ATTN CHIEF, ENGINEERING SCIENCES

US ARMY RESEARCH OFFICE
P. O. BOX 12211
RESEARCH TRIANGLE PARK, NC 27709
ATTN JAMES J. MURRAY, ENG SCI DIV

BMD ADVANCED TECHNOLOGY CENTER
P.O. BOX 1500
HUNTSVILLE, AL 35807
ATTN J. PAPADOPOULOS

COMMANDER
USA FOREIGN SCIENCE & TECHNOLOGY CENTER
FEDERAL OFFICE BUILDING
220 7th STREET, NE
CHARLOTTESVILLE, VA 22901
ATTN DRXST-SD1

DIRECTOR
APPLIED TECHNOLOGY LABORATORY
FORT EUSTIS, VA 23604
ATTN GEORGE W. FOSDICK, DAVDL-EU-SYA

COMMANDER
USA MISSILE RES & DEV COMMAND
REDSTONE ARSENAL, AL 35809
ATTN REDSTONE SCIENTIFIC INFORMATION
CENTER, DRSMI-RBD
ATTN DRDMI-TGC, WILLIAM GRIFFITH
ATTN DRDMI-TGC, J. C. DUNAWAY
ATTN DRCPM-TOE, FRED J. CHEPLEN

COMMANDER
USA MOBILITY EQUIPMENT R&D CENTER
FORT BELVOIR, VA 22060
ATTN TECHNICAL LIBRARY (VAULT)
ATTN DRDME-EM, R. N. WARE

COMMANDER
EDGEWOOD ARSENAL
ABERDEEN PROVING GROUND, MD 21010
ATTN SAREA-MT-T, MR. D. PATTON

COMMANDER
US ARMY ARRADCOM
DOVER, NJ 07801
ATTN SARPA-TS-S-#59
ATTN DRDAR-LCN-F, A. E. SCHMIDLIN
ATTN DRDAR-LCW-E, MR. J. CONNOR

COMMANDER
WATERVLIET ARSENAL
WATERVLIET ARSENAL, NY 12189
ATTN SARWV-RDT-L

COMMANDER
USA TANK AUTOMOTIVE RES & DEV COMMAND
ARMOR & COMP DIV, DRDTA-RKT
BLDG 215
WARREN, MI 48090
ATTN T. KOZOWYK
ATTN M. STEELE

COMMANDER
WHITE SANDS MISSILE RANGE, NM 88002
ATTN STEWS-AD-L, TECHNICAL LIBRARY

COMMANDER
US ARMY ARMAMENT MATERIEL
READINESS COMMAND
ROCK ISLAND, IL
ATTN DRSAR-RDG-T, MR. R. SPENCER
ATTN DRSAR-ASF
ATTN DRSAR-LEP-L, TECHNICAL LIBRARY

COMMANDER/DIRECTOR
ATMOSPHERIC SCIENCES LABORATORY
USA ERADCOM
WHITE SANDS MISSILE RANGE, NM 88002
ATTN DELAS-AS (HOLT)

OFFICE OF NAVAL RESEARCH
DEPARTMENT OF THE NAVY
ARLINGTON, VA 22217
ATTN STANLEY W. DOROFF, CODE 438
ATTN D. S. SIEGEL, CODE 211

DEPARTMENT OF THE NAVY
R&D PLANS DIVISION
ROOM 5D760, PENTAGON
WASHINGTON, DC 20350
ATTN BENJ F. PETRIE, JR.
OP-987P4

COMMANDER
NAVAL AIR DEVELOPMENT CENTER
WARMINSTER, PA 18974
ATTN R. MCGIBONEY, 30424
ATTN CODE 8134, LOIS GUISE

NAVAL AIR SYSTEMS COMMAND
DEPARTMENT OF THE NAVY
WASHINGTON, DC 20360
ATTN CODE AIR-52022A, J. BURNS
ATTN CODE AIR-52022E, D. HOUCK

COMMANDER
PACIFIC MISSILE RANGE
NAVAL MISSILE CENTER
POINT MUGU, CA 93042
ATTN CODE 3123, ABE J. GARRETT
ATTN CODE 1243, A. ANDERSON

COMMANDER
NAVAL SHIP ENGINEERING CENTER
PHILADELPHIA DIVISION
PHILADELPHIA, PA 19112
ATTN CODE 6772, D. KEYSER

COMMMANDER
NAVAL SURFACE WEAPONS CENTER
WHITE OAK, MD 20910
ATTN CODE 413, CLAYTON MCKINDRA
ATTN CODE WA-33, J. O'STEEN

COMMANDER
NAVAL ORDNANCE STATION
INDIANHEAD, MD 20640
ATTN CODE 5123B, J. MORRIS

NAVAL SHIP RES & DEV CENTER
CODE 1619, MR. K. READER
BETHESDA, MD 20084

NAVAL SEA SYSTEMS COMMAND
SEA0331H
WASHINGTON, DC 20362
ATTN A. CHAIKIN

COMMANDER
NAVAL WEAPONS CENTER
CHINA LAKE, CA 93555
ATTN CODE 533, LIBRARY DIVISION
ATTN CODE 5536, MR. M. D. JACOBSON

COMMANDER
AF AERO PROPULSION LABORATORY, AFSC
WRIGHT-PATTERSON AFB, OH 45433
ATTN LESTER SMALL 1TBC

COMMANDER
AIR FORCE AVIONICS LABORATORY
WRIGHT-PATTERSON AFB, OH 45433
ATTN RWN-2, RICHARD JACOBS

DIRECTOR
AF OFFICE OF SCIENTIFIC RESEARCH
1400 WILSON BLVD
ARLINGTON, VA 22209
ATTN NE, MR.GEORGE KNAUSENBERGER

COMMANDER
AIR FORCE FLIGHT DYNAMICS LABORATORY
WRIGHT-PATTERSON AFB, OH 45433
ATTN AFFDL/FGL, H. SNOWBALL

COMMANDER
AF WEAPONS LABORATORY, AFSC
KIRTLAND AFB, NM 87117
ATTN SUL, TECHNICAL LIBRARY

COMMANDER
ARMAMENT DEVELOPMENT AND TEST CENTER
EGLIN AIR FORCE BASE, FL 32542
ATTN ADTC (DLOSL), TECH LIBRARY

AIR FORCE FLIGHT TEST CENTER
6510 ABG/SSD
EDWARDS AFB, CA 93523
ATTN TECHNICAL LIBRARY

AF INSTITUTE OF TECHNOLOGY, AU
WRIGHT-PATTERSON AFB, OH 45433
ATTN LIBRARY AFIT(LD),
BLDG 640, AREA B
ATTN AFIT(ENM), MILTON E. FRANKE

AEROSPACE MEDICAL DIVISION
BROOKS AFB, TX 78235
ATTN AMD/RDN, CPT G. JAMES

DIV. OF REACTOR RES & DEV
F-309 USERDA
WASHINGTON, DC 20545
ATTN FRANK C. LEGLER

OAK RIDGE NATIONAL LABORATORY
CENTRAL RES LIBRARY,
BLDG 4500N, RM 175
P. O. BOX X
OAK RIDGE, TN 37830
ATTN E. HOWARD

DEPT OF HEW
PUBLIC HEALTH SERVICE
NATIONAL INSTITUTE OF HEALTH
BLDG 13, RM 3W-13
BETHESDA, MD 20014
ATTN C. J. MCCARTHY

DEPARTMENT OF COMMERCE
NATIONAL BUREAU OF STANDARDS
WASHINGTON, DC 20234
ATTN DR. JAMES SCHOOLEY, CHIEF,
TEMPERATURE SECTION
ATTN DR. T. NEGAS, MATERIALS DIVISION

DEPARTMENT OF COMMERCE
BUREAU OF EAST-WEST TRADE
OFFICE OF EXPORT ADMINISTRATION
WASHINGTON, DC 20230
ATTN WALTER J. RUSNACK

SCIENTIFIC LIBRARY
US PATENT OFFICE
WASHINGTON, DC 20231
ATTN MRS. CURETON

DEPARTMENT OF COMMERCE
NATIONAL BUREAU OF STANDARDS
WASHINGTON, DC 20234
ATTN GUSTAVE SHAPIRO, 425.00

NASA AMES RESEARCH CENTER
MOFFETT FIELD, CA 94035
ATTN MS 244-13, DEAN CHISEL

NASA LANGLEY RESEARCH CENTER
HAMPTON, VA 23665
ATTN MS 494, H. D. GARNER
ATTN MS 494, R. R. HELLBAUM
ATTN MS 185, TECHNICAL LIBRARY

NASA LEWIS RESEARCH CENTER
21000 BROOKPARK ROAD
CLEVELAND, OH 44135
ATTN VERNON D. GEBBEN

NASA SCIENTIFIC & TECH INFO FACILITY
P. O. BOX 8657
BALTIMORE/WASHINGTON INTERNATIONAL
AIRPORT, MD 21240
ATTN ACQUISITIONS BRANCH

UNIVERSITY OF ALABAMA
CIVIL & MINERAL ENGINEERING DEPT.
P. O. BOX 1468
UNIVERSITY, AL 35486
ATTN DR. HAROLD R. HENRY

ARIZONA STATE UNIVERSITY
ENGINEERING CENTER
TEMPE, AZ 85281
ATTN PETER K. STEIN, LABORATORY
FOR MEASUREMENT SYSTEMS ENGR.

UNIVERSITY OF ARKANSAS
TECHNOLOGY CAMPUS
P. O. BOX 3017
LITTLE ROCK, AR 72203
ATTN PAUL C. MCLEOD

UNIVERSITY OF ARKANSAS
MECHANICAL ENGINEERING
FAYETTEVILLE, AR 72701
ATTN JACK H. COLE, ASSOC PROF

CARNEGIE-MELLON UNIVERSITY
SCHENLEY PARK
PITTSBURGH, PA 15213
ATTN PROF W. T. ROULEAU, MECH ENGR DEPT

CASE WESTERN RESERVE UNIVERSITY
UNIVERSITY CIRCLE
CLEVELAND, OH 44106
ATTN PROF P. A. ORNER

DISTRIBUTION (Cont'd)

THE CITY COLLEGE OF THE CITY
UNIVERSITY OF NY
DEPT OF MECH ENGR
139th ST. AT CONVENT AVE
NEW YORK, NY 10031
ATTN PROF L. JIJI
ATTN PROF G. LOWEN

DUKE UNIVERSITY
COLLEGE OF ENGINEERING
DURHAM, NC 27706
ATTN C. M. HARMAN

ENGINEERING SOCIETIES LIBRARY
345 EAST 47TH STREET
NEW YORK, NY 10017
ATTN HOWARD GORDON
ATTN ACQUISITIONS DEPARTMENT

FRANKLIN INSTITUTE OF THE STATE
OF PENNSYLVANIA
20TH STREET & PARKWAY
PHILADELPHIA, PA 19103
ATTN KA-CHEUNG TSUI, ELEC ENGR DIV
ATTN C. A. BELSTERLING

HUGHES HELICOPTERS
DIVISION OF SUMMA CORPORATION
CENTINELA & TEALE STREETS
CULVER CITY, CA 90230
ATTN LIBRARY 2/T2124

IIT RESEARCH INSTITUTE
10 WEST 35th STREET
CHICAGO, IL 60616
ATTN DR. K. F. MCKEE

JOHNS HOPKINS UNIVERSITY
APPLIED PHYSICS LABORATORIES
LAUREL, MD 20810
ATTN MR. MAYNARD HILL
ATTN MR. THOMAS RANKIN
ATTN MR. JOSEPH WALL

LEHIGH UNIVERSITY
DEPARTMENT OF MECHANICAL ENGINEERING
BETHLEHEM, PA 18015
ATTN PROF FORBES T. BROWN

LINDA HALL LIBRARY
5109 CHERRY STREET
KANSAS CITY, MO 64110
ATTN DOCUMENTS DIVISION

MASSACHUSETTS INSTITUTE OF TECHNOLOGY
77 MASSACHUSETTS AVENUE
CAMBRIDGE, MA 02139
ATTN ENGINEERING TECHNICAL REPORTS,
RM 10-408
ATTN DAVID WORMLEY, MECH ENGR DEPT,
RM 3-146

MICHIGAN TECHNOLOGICAL UNIVERSITY
LIBRARY, DOCUMENTS DIVISION
HOUGHTON, MI 49931
ATTN J. HAWTHORNE

UNIVERSITY OF MISSISSIPPI
201 CARRIER HALL, DEPT OF MECH ENGR
UNIVERSITY, MS 38677
ATTN DR. JOHN A. FOX

MISSISSIPPI STATE UNIVERSITY
DRAWER ME
STATE COLLEGE, MS 39672
ATTN DR. C. J. BELL, MECH ENG DEPT

UNIVERSITY OF NEBRASKA LIBRARIES
ACQUISITIONS DEPT, SERIALS SECTION
LINCOLN, NE 68508
ATTN ALAN GOULD

UNIVERSITY OF NEW HAMPSHIRE
MECH ENGR DEPT, KINGSBURY HALL
DURHAM, NH 03824
ATTN PROF CHARLES TATE

DEPARTMENT OF MECHANICAL ENGINEERING
NEWARK COLLEGE OF ENGINEERING
323 HIGH STREET
NEWARK, NJ 07102
ATTN DR. R. Y. CHEN

OHIO STATE UNIVERSITY LIBRARIES
SERIAL DIVISION, MAIN LIBRARY
1858 NEIL AVENUE
COLUMBUS, OH 43210

OKLAHOMA STATE UNIVERSITY
SCHOOL OF MECH & AEROSPACE ENGR.
STILLWATER, OK 74074
ATTN PROF KARL N. REID

MIAMI UNIVERSITY
DEPT OF ENG TECH
SCHOOL OF APPLIED SCIENCE
OXFORD, OH 45056
ATTN PROF S. B. FRIEDMAN

PENNSYLVANIA STATE UNIVERSITY
215 MECHANICAL ENGINEERING BUILDING
UNIVERSITY PARK, PA 16802
ATTN DR. J. L. SHEARER

PENNSYLVANIA STATE UNIVERSITY
ENGINEERING LIBRARY
201 HAMMOND BLDG
UNIVERSITY PARK, PA 16802
ATTN M. BENNETT, ENGINEERING LIBRARIAN

DISTRIBUTION (Cont'd)

PURDUE UNIVERSITY
SCHOOL OF MECHANICAL ENGINEERING
LAFAYETTE, IN 47907
ATTN PROF. VICTOR W. GOLDSCHMIDT
ATTN PROF. ALAN T. MCDONALD

ROCK VALLEY COLLEGE
3301 NORTH MULFORD ROAD
ROCKFORD, IL 61101
ATTN KEN BARTON

RUTGERS UNIVERSITY
LIBRARY OF SCIENCE & MEDICINE
NEW BRUNSWICK, NJ 08903
ATTN GOVERNMENT DOCUMENTS DEPT
MS. SANDRA R. LIVINGSTON

SYRACUSE UNIVERSITY
DEPT OF MECH & AEROSPACE ENGINEERING
139 E. A. LINK HALL
SYRACUSE, NY 13210
ATTN PROFESSOR D. S. DOSANJH

UNIVERSITY OF TEXAS AT AUSTIN
DEPT OF MECHANICAL ENGINEERING
AUSTIN, TX 78712
ATTN DR. A. J. HEALEY

THE UNIVERSITY OF TEXAS AT ARLINGTON
MECHANICAL ENGINEERING DEPARTMENT
ARLINGTON, TX 76019
ATTN DR. ROBERT L. WOODS

TULANE UNIVERSITY
DEPT OF MECHANICAL ENGINEERING
NEW ORLEANS, LA 70118
ATTN H. F. HRUBECKY

UNION COLLEGE
MECHANICAL ENGINEERING
SCHENECTADY, NY 12308
ATTN ASSOC PROF W. C. AUBREY
MECH ENGR DEPT, STEINMETZ HALL

VIRGINIA POLYTECHNIC INSTITUTE OF STATE UNIV
MECHANICAL ENGINEERING DEPARTMENT
BLACKSBURG, VA 24061
ATTN PROF H. MOSES

WASHINGTON UNIVERSITY
SCHOOL OF ENGINEERING
P. O. BOX 1185
ST. LOUIS, MO 63130
ATTN W. M. SWANSON

WEST VIRGINIA UNIVERSITY
MECHANICAL ENGINEERING DEPARTMENT
MORGANTOWN, WV 26505
ATTN DR. RICHARD A. BAJURA

WICHITA STATE UNIVERSITY
WICHITA, KS 67208
ATTN DEPT AERO ENGR, E. J. RODGERS

UNIVERSITY OF WISCONSIN
MECHANICAL ENGINEERING DEPARTMENT
1513 UNIVERSITY AVENUE
MADISON, WI 53706
ATTN FEDERAL REPORTS CENTER
ATTN NORMAN H. BEACHLEY, DIR,
DESIGN ENGINEERING LABORATORIES

WORCESTER POLYTECHNIC INSTITUTE
WORCESTER, MA 01609
ATTN GEORGE C. GORDON LIBRARY (TR)
ATTN TECHNICAL REPORTS

AIRESEARCH
P. O. BOX 5217
402 SOUTH 36th STREET
PHOENIX, AZ 85034
ATTN DAVID SCHAFFER
ATTN TREVOR SUTTON
ATTN TOM TIPPETTS

AVCO SYSTEMS DIVISION
201 LOWELL STREET
WILMINGTON, MA 01887
ATTN W. K. CLARK

BELL HELICOPTER COMPANY
P. O. BOX 482
FORTWORTH, TX 76101
ATTN MR. R. D. YEARY

BENDIX CORPORATION
ELECTRODYNAMICS DIVISION
11600 SHERMAN WAY
N. HOLLYWOOD, CA 90605
ATTN MR. D. COOPER

BENDIX CORPORATION
RESEARCH LABORATORIES DIV.
BENDIX CENTER
SOUTHFIELD, MI 48075
ATTN C. J. AHERN

BOEING COMPANY, THE
P. O. BOX 3707
SEATTLE, WA 98124
ATTN HENRIK STRAUB

BOWLES FLUIDICS CORPORATION
9347 FRASER AVENUE
SILVER SPRING, MD 20910
ATTN VICE PRES./ENGR.

DR. RONALD BOWLES
2105 SONDRA COURT
SILVER SPRING, MD 20904

DISTRIBUTION (Cont'd)

CONTINENTAL CAN COMPANY
TECH CENTER
1350 W. 76TH STREET
CHICAGO, IL 60620
ATTN P. A. BAUER

CORDIS CORPORATION
P. O. BOX 428
MIAMI, FL 33137
ATTN STEPHEN F. VADAS, K-2

CORNING GLASS WORKS
FLUIDIC PRODUCTS
HOUGHTON PARK, B-2
CORNING, NY 14830
ATTN MR. W. SCHEMERHORN

CHRYSLER CORPORATION
P.O. BOX 118
CIMS-418-33-22
DETROIT, MI 48231
ATTN MR. L. GAU

EMX ENGINEERING, INC
BOX 216 - 216 LITTLE FALLS RD
CEDAR GROVE, NJ 07009
ATTN ANTHONY P. CORRADO, PRESIDENT

FLUIDICS QUARTERLY
P. O. BOX 2989
STANFORD, CA 94305
ATTN D. H. TARUMOTO

GENERAL ELECTRIC COMPANY
SPACE/RESD DIVISIONS
P. O. BOX 8555
PHILADELPHIA, PA 19101
ATTN MGR LIBRARIES, LARRY CHASEN

GENERAL MOTORS CORPORATION
DELCO ELECTRONICS DIV
MANFRED G. WRIGHT
NEW COMMERCIAL PRODUCTS
P. O. BOX 1104
KOKOMO, IN 46901
ATTN R. E. SPARKS

GRUMMAN AEROSPACE CORPORATION
TECHNICAL INFORMATION CENTER
SOUTH OYSTER BAY ROAD
BETHPAGE, L. I., NY 11714
ATTN C. W. TURNER, DOCUMENTS
LIBRARIAN

HAMILTON STANDARD
DIVISION OF UNITED AIRCRAFT
CORPORATION
WINDSOR LOCKS, CT 06096
ATTN MR. PHILIP BARNES

HONEYWELL, INC.
1625 ZARTHAN AVE
MINNEAPOLIS, MI 55413
ATTN J. HEDEEN

JOHNSON CONTROLS, INC
507 E. MICHIGAN
MILWAUKEE, WI 53201
ATTN WARREN A. LEDERMAN

MOORE PRODUCTS COMPANY
SPRING HOUSE, PA 19477
ATTN MR. R. ADAMS

MARTIN MARIETTA CORPORATION
AEROSPACE DIVISION
P. O. BOX 5837
ORLANDO, FL 32805
ATTN R. K. BRODERSON, MP 326
ATTN VITO O. BRAVO, MP 326

MCDONNELL AIRCRAFT COMPANY
GUIDANCE AND CONTROL MECHANICS DIVISION
ST. LOUIS, MO 63166
ATTN MR. LOYAL GUENTHER

NATIONAL FLUID POWER ASSOCIATION
3333 NORTH MAYFAIR ROAD
MILWAUKEE, WI 53222
ATTN JOHN R. LUEKE
DIR OF TECH SERVICES

PLESSEY AEROSPACE LTD
500 NORTHWEST PLAZA
SUITE 814
ST. ANN, MO 63074
ATTN MR. GEORGE UPTON

RICHARD WHITE & ASSOCIATES
ELECTRO/MECHANICAL ENGINEERS
77 PELHAM ISLE ROAD
SUDSBURY, MA 01776
ATTN RICHARD P. WHITE

ROCKWELL INTERNATIONAL CORPORATION
COLUMBUS AIRCRAFT DIVISION, P. O. BOX 1259
4300 E. 5TH AVENUE
COLUMBUS, OH 43216
ATTN MR. MARVIN SCHWEIGER

SANDIA CORPORATION
KIRTLAND AFB, EAST
ALBUQUERQUE, NM 87115
ATTN WILLIAM R. LEUENBERGER, DIV 2323

TRITEC, INC
P.O. BOX 56
COLUMBIA, MD 21045
ATTN L. SIERACKI

DISTRIBUTION (Cont'd)

UNITED TECHNOLOGIES RESEARCH CENTER
400 MAIN STREET
E. HARTFORD, CT 06108
ATTN R. E. OLSON, MGR FLUID
DYNAMICS LABORATORY

US ARMY ELECTRONICS RESEARCH
& DEVELOPMENT COMMAND
ATTN WISEMAN, ROBERT S., DR., DRDEL-CT

HARRY DIAMOND LABORATORIES
ATTN 00100, COMMANDER/TECH DIR/TSO
ATTN CHIEF, DIV 10000
ATTN CHIEF, DIV 20000
ATTN CHIEF, DIV 30000
ATTN CHIEF, DIV 40000
ATTN RECORD COPY, 81200
ATTN HDL LIBRARY, 81100 (3 COPIES)
ATTN HDL LIBRARY, 81100 (WOODBRIDGE)
ATTN TECHNICAL REPORTS BRANCH, 81300
ATTN CHAIRMAN, EDITORIAL COMMITTEE
ATTN COX, L. S. 00210
ATTN EITNER, B. PAO
ATTN CHIEF, 13000
ATTN LANHAM, C 00210
ATTN DRZEWIECKI, T. 13400
ATTN GOTO, J. 13400
ATTN HOLMES, A. 13400 (5 COPIES)
ATTN GEHMAN, S. 13400 (5 COPIES)
ATTN CHIEF, 13400 (10 COPIES)

AD-A075 206 HARRY DIAMOND LABS ADELPHI MD F/G 13/7
A FLUIDIC APPROACH TO THE DESIGN OF A MUD PULSER FOR BORE-HOLE --ETC(U)
AUG 79 A B HOLMES , S E GEHAMAN
UNCLASSIFIED HDL-TM-79-21 NL

2 OF 2

AD A075206

END
DATE FILMED
10-80
DTIC

SUPPLEMENTARY

INFORMATION

DEPARTMENT OF THE ARMY
HARRY DIAMOND LABORATORIES
2800 POWDER MILL ROAD
ADELPHI, MD. 20783

DELHD-TIA-R

25 June 1980

SUBJECT: Errata Sheet to HDL-TM-79-21, A Fluidic Approach to the Design of a Mud Pulser for Bore-Hole Telemetry While Drilling, dated August 1979, by Allen B. Holmes and Stacy E. Gehman

TO: Recipients of HDL-TM-79-21

The enclosed page should be substituted for page 25/26 of subject report.

FOR THE COMMANDER:

RUTH E. SAVAGE
Chief, Technical Reports Branch

1 Incl
as

where

$$1/K_{13}^2 = \left(1/K_1^2\right) + \left(1/K_3^2\right)$$

and

$$1/K_{23}^2 = \left(1/K_2^2\right) + \left(1/K_3^2\right) .$$

If we define

$$a = \frac{1}{K_{23}^2} - \frac{1}{K_{13}^2} ,$$

$$b = \frac{2}{K} + \frac{4Q}{K_{13}^2} , \quad \text{and}$$

$$c = -\left(\frac{4Q^2}{K_{13}^2} + \frac{2Q}{K}\right)$$

then Q_2 is given by

$$Q_2 = \frac{-b + \sqrt{b^2 - 4ac}}{2a} . \tag{15}$$

From equations (8) through (13), the following relationships can be found.

$$Q_1 = 2Q - Q_2 \tag{16}$$

$$P_{B1} = Q_1^2/K_3^2 \tag{17}$$

$$P_{B2} = Q_2^2/K_{32}^2 \tag{18}$$

$$P_1 = Q_1^2/K_{13}^2 \tag{19}$$

$$P_2 = Q_2^2/K_{23}^2 \tag{20}$$

Thus, given the effective areas of the mud pulser (A_1 and A_2), the bit area (A_3), the mud density (ρ), and the average flow rate through the pulser (determined by the flow rate (Q) at the pump), it is possible to calculate the dynamic downhole conditions. The results of such a calculation are shown in table II along with calculations of the steady-state pressure that would be expected if the pulser were closer to the mud pump or if it were steadily operated in either the easy or hard direction. The relationships in table II apply to any mud pulser in which the area changes are as indicated.

TABLE II. PULSER DYNAMIC PERFORMANCE

Drill pipe ID = 3.75 in. (9.52 cm)
Bit area = 0.35 $in.^2$ (2.26 cm^2)
Mud density = 10 ppg (1198 kg/m^3)
Sound speed = 4710 ft/s (1435 m/s)
Easy pulser area, $A1_{eff}$ = 1.0 $in.^2$ (6.45 cm^2)

Average circulation flow rate (gal/min)[a]	Pulser operating conditions[b]										
	Steady state				Dynamic						
	Bit pressure (psi)[c]	Upstream pressure (psi)[c]		Signal pressure (psi)[c]	Flow rate (gal/min)[a]		Bit pressure (psi)[c]		Upstream pressure (psi)[c]		Signal pressure (psi)[c]
		Hard	Easy		Hard	Easy	Hard	Easy	Hard	Easy	
For flow rate = 100	75	108	83	25	97	103	70	79	102	88	14
200	299	432	332	100	192	208	275	324	397	360	37
400	1197	1728	1329	401	380	420	1078	1321	1557	1468	89
$A2_{eff}$ = 0.5 $in.^2$ (3.2 cm^2) (Turndown = 2)											
For flow rate = 100	75	208	83	125	88	112	57	94	159	105	54
200	299	831	332	499	168	232	211	402	587	447	140
400	1197	3322	1329	1993	325	475	792	1684	2200	1871	329
$A2_{eff}$ = 0.25 $in.^2$ (1.6 cm^2) (Turndown = 4)											

[a] *(ft/s)0.3048 = (m/s)*

[b] *All pressures are referenced to dowhnhole pressure*

[c] *(psi)6.895 = (kPa)*

Examination of table II shows that the dynamic signal pressure (water hammer) is much less than would be expected from steady-state operating characteristics. However, if the turndown ratio is greater than 2 and the flow rate is 200 gal/min* or higher, then the dynamic signal pressure is at least 37 psi.

Use of calculations such as these allows pulser size and turndown ratios to be optimized for a given bit area and mud flow rate. Accurate calculations of downhole conditions are also necessary for valid interpretation of field-test data.

*$(gal/min)6.31 \times 10^{-5} = m^3/s$.